

Molecular Rotors: Design, Synthesis, Structural Analysis, and Silver Complex of New [7.7]Cyclophanes

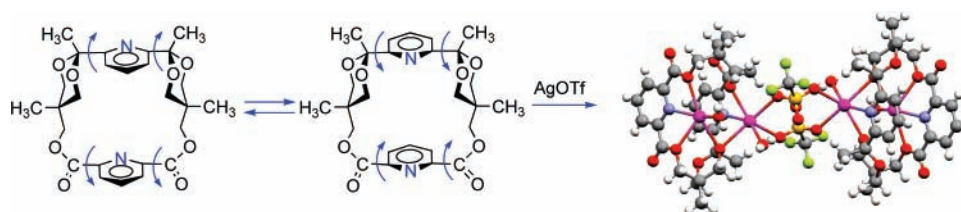
Niculina Bogdan,^{†,‡} Ion Grosu,^{*,†} Guillaume Benoît,[‡] Loïc Toupet,[§]
Yvan Ramondenc,[‡] Eric Condamine,[‡] Ioan Silaghi-Dumitrescu,[†] and Gérard Plé[‡]

“Babes-Bolyai” University, Faculty of Chemistry and Chemical Engineering,
11 Arany Janos str., 400028 Cluj-Napoca, Romania, Université de Rouen, IRCOF,
UMR 6014, Faculté des Sciences, 76821 Mont Saint-Aignan, Cedex, France, and
Université de Rennes I, UMR C 6626, 35042 Rennes, Cedex, France

igrosu@chem.ubbcluj.ro

Received May 3, 2006

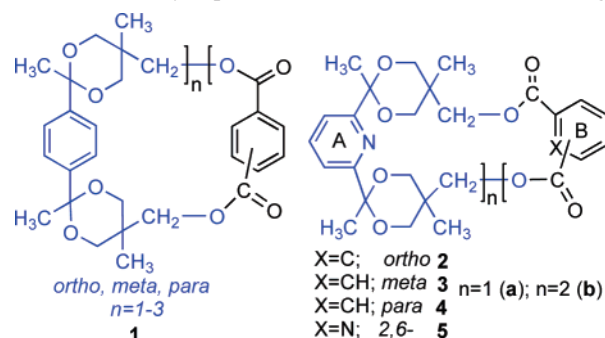
ABSTRACT



New molecular rotors, [7.7](2,6)pyridinocyclophanes (monomers and dimers) embedding 1,3-dioxanes in the bridges, were investigated by variable-temperature NMR, molecular modeling, and single-crystal X-ray diffractometry. The nitrogen-inside rotation of the pyridine ring is more hindered in the derivatives with longer distance between the bridges (i.e., para > meta and 2,6-pyridylene > ortho) and can be chemically stopped by complexation with CF₃SO₃Ag.

Cyclophanes are bridged aromatic compounds and they represent attractive synthetic targets due to their intriguing chemical, physicochemical, and biological properties.¹ The total synthesis of some naturally occurring [7.7]cyclophanes,² reported to have cytoactivity,³ was recently disclosed. Recent literature data reveals an increasing interest in cyclophanes with cavities of varying sizes, as molecular “hosts”.⁴ Many of these cyclophanes are also investigated as molecular rotors.⁵ The efficient synthesis of large cyclophanes requires the favorable preorganization⁶ of the substrate for the closure of the macrocycle. In a previous work,⁷ we reported the high-yielding synthesis of new [7.7]cyclophanes (**1** in Chart 1)

Chart 1. [7.7]Cyclophanes with 1,3-Dioxane Units as Bridges



[†] “Babes-Bolyai” University.

[‡] Université de Rouen.

[§] Université de Rennes I.

(1) (a) Weber, E. *Cyclophanes*. In *Topics in Current Chemistry*; Springer-Verlag: Berlin, 1994; Vol. 172. (b) Vögtle, F. *Cyclophane Chemistry: Synthesis, Structures and Reactions*; John Wiley and Sons: Chichester, 1993. (d) Gleiter, R.; Hopf, H. *Modern Cyclophane Chemistry*; Wiley-VCH Verlag GmbH & Co. KGaA: Weinheim, 2004.

from appropriately substituted 1,3-dioxane derivatives of 1,4-diacetylbenzene.

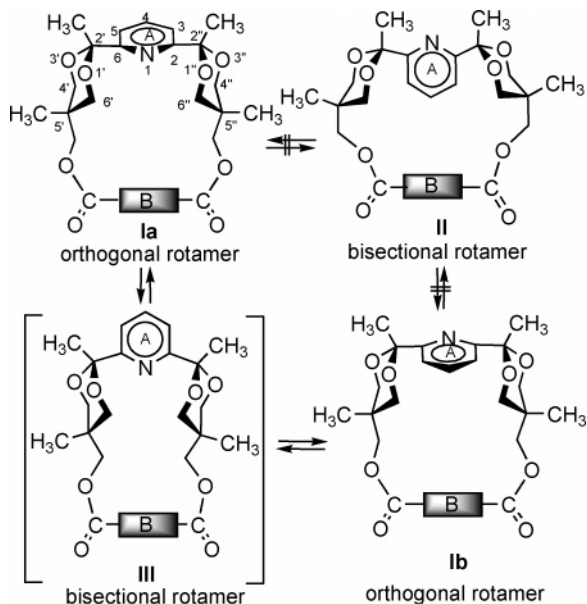
Similarly to the 1,3-dioxane derivatives of 1,4-diacetylbenzene,⁸ the analogous derivatives of 2,6-diacetylpyridine⁹

display a favorable stereochemistry (i.e., axial orientation of the aromatic ring relative to both saturated heterocycles) for macrocyclization to generate cyclophanes. We considered it of interest to prepare the (2,6)pyridinocyclophanes **2–5**, embedding the 2,6-bis(2-methyl-1,3-dioxan-2-yl)pyridine moiety (Chart 1), and to elucidate their stereochemistry and supramolecular properties and the dynamics of the pyridine ring within the macrocycle.

(2,6)-Pyridinocyclophanes **2–5** were obtained in good yields by reacting the appropriate 1,3-dioxanediol [*cis*-2,*cis*-6-bis(2,5-dimethyl-5(*r*)-hydroxymethyl-1,3-dioxan-2-yl)pyridine], previously synthesized from 2,6-diacetylpyridine by the ketalization, with different aromatic dicarboxylic acid dichlorides.

The NMR investigations in solution, the single-crystal X-ray diffraction molecular structures for compounds **2a** and **5a**, as well as the molecular modeling performed on all the newly synthesized cyclophanes showed the high preference of these compounds for the conformers in which the 2,6-disubstituted pyridine ring (denoted as **A**, Chart 1 and Scheme 1) adopts an axial-orthogonal orientation with respect

Scheme 1. Rotation of 2,6-Pyridylene Ring in **2a–5a**



to both 1,3-dioxane rings and the other aromatic unit (denoted as **B**) is slightly tilted to the ring A (X-ray A/B dihedral angles are in the range: 24.50–32.09°). The cyclophanes

(2) (a) Smith, A. B., III; Kozmin, S. A.; Adams, C. M.; Paone, D. V. *J. Am. Chem. Soc.* **2000**, *122*, 4984–4985. (b) Smith, A. B., III; Kozmin, S. A.; Paone, D. V. *J. Am. Chem. Soc.* **1999**, *121*, 7423–7424. (c) Smith, A. B., III; Adams, C. M.; Kozmin, S. A.; Paone, D. V. *J. Am. Chem. Soc.* **2001**, *123*, 5925–5937.

(3) Moore, B. S.; Chen, J. L.; Patterson, G. M. L.; Moore, R. E.; Brinen, L. S.; Kato, Y.; Clardy, L. *J. Am. Chem. Soc.* **1990**, *112*, 4061–4063.

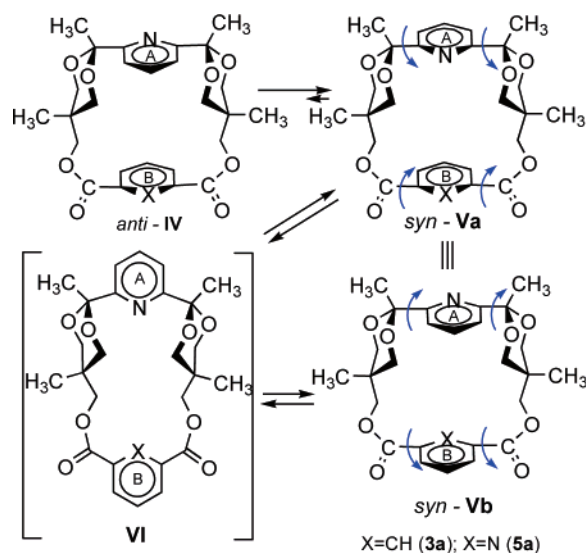
(4) (a) Lukyanenko, N. G.; Kirichenko, T. I.; Lyapunov, A. Y.; Mazepa, A. V.; Simonov, Y. A.; Fonari, M. S.; Botoshansky, M. M. *Chem. Eur. J.* **2005**, *11*, 262–270. (b) Hahn, D.-W.; Byun, D.-M.; Tae, J. *Eur. J. Org. Chem.* **2005**, 63–67. (c) Pia, E.; Toba, R.; Chas, M.; Peinador, C.; Quintela, J. M. *Tetrahedron Lett.* **2006**, 1953–1956.

2–5 are excellent models to investigate the rotation of the pyridine ring (**A**) relative to the macrocycle (Scheme 1).

Molecular modeling showed a limited degree of rotation for ring **A**; in all four cases only a half-rotation (180°) is favorable. The calculations revealed a significantly higher barrier for the transformation **Ia** ⇌ **II** ⇌ **Ib** than for the rotation of the pyridine ring **A** involving conformer **III**, with the nitrogen atom “inside” the macrocycle (**Ia** ⇌ **III** ⇌ **Ib**; see the Supporting Information). Due to this hindered rotation, the ring **A** exhibits an oscillation movement similar to the work of a rudder.

The conformational behavior is somewhat more complex for **3a** and **5a**. The pyridine ring **A** and the other aromatic group (**B**, Scheme 2) can have syn or anti orientations. In

Scheme 2. Concerted Rotation of the Aromatic Rings in **3a** and **5a**



the syn orientation, the N atom of ring **A** and the X group of ring **B** (X = N atom for **5a** or X = CH for **3a**) are located on the same side of the best plane of the 1,3-dioxane rings.¹⁰ The molecular modeling found the syn structure to be considerably more stable than the anti conformer, predicting thus the syn rotamer to be predominant in these compounds [$\Delta G^{\circ}_{\text{anti-syn}}$ (**3a**) = 8.37 and $\Delta G^{\circ}_{\text{anti-syn}}$ (**5a**) = 7.72 kcal/mol]. Molecular dynamics simulations revealed that a tandem disrotatory half-rotation of the two aromatic rings **A** and **B**

(5) (a) Kottas, G. S.; Clarke, L. I.; Horinek, D.; Michl, J. *Chem. Rev.* **2005**, *105*, 1281–1376. (b) Hirata, O.; Takeuchi, M.; Shinkai, S. *Chem. Commun.* **2005**, 3805–3807. (c) Alfonso, I.; Burguete, M. I.; Luis, S. V. *J. Org. Chem.* **2006**, *71*, 2242–2250. (d) Kanazawa, H.; Higuchi, M.; Yamamoto, K. *J. Am. Chem. Soc.* **2005**, *127*, 16404–16405.

(6) (a) Blankenstein, J.; Zhu, J. *Eur. J. Org. Chem.* **2005**, 1949–1964. (b) Steed, J. W.; Atwood, J. L. *Supramolecular Chemistry*; John Wiley and Sons: Chichester, 2000; p 91.

(7) Balog, M.; Grosu, I.; Plé, G.; Ramondenc, Y.; Condamine, E.; Varga, R. A. *J. Org. Chem.* **2004**, *69*, 1337–1345.

(8) Grosu, I.; Muntean, L.; Toupet, L.; Plé, G.; Pop, M.; Balog, M.; Mager, S.; Bogdan, E. *Monatsh. Chem.* **2002**, *133*, 631–641.

(9) Balog, M.; Tötös, S.; Florian, C. M.; Grosu, I.; Plé, G.; Toupet, L.; Ramondenc, Y.; Dinca, N. *Heterocycl. Commun.* **2004**, *10*, 139–144.

(10) The best plane of the 1,3-dioxane ring is the plane C²C^{2''}C^{5'}C^{5''}.

occurs in **3a** and **5a** (Scheme 2). The concerted rotation of the two aromatic rings is similar to the work of a *wringer*.

Variable-temperature NMR experiments exhibit major differences between the spectra of mobile (i.e., fast conformational equilibrium) and frozen (2,6)pyridinocyclophanes. The ^1H NMR spectra of the frozen conformers are complex and display distinct signals for the diastereotopic groups (e.g., the two CH_2 groups of each 1,3-dioxane ring are rendered diastereotopic by the planar chirality of the frozen, syn cyclophanes), whereas the spectra of the mobile molecules show isochronous signals for these groups, which are rendered equivalent by the fast rotation of the pyridine ring (**A**).

The variable-temperature NMR experiments (Table 1) reveal significantly different temperature profiles for

Table 1. Variable-Temperature NMR Data (δ , ppm, CDCl_3) for **2a–5a** and **4b**

rotor ^a	<i>T</i> (K)	δ_{axial}		$\delta_{\text{equatorial}}$		
		4(4')	6(6')	4'(4'')	6'(6'')	
4a	S	293	3.97	4.05	3.79	4.16
4b	W	295 ^b	3.86		3.67	
4b	S	180 ^b	3.18–4.20 ^d			
3a	W	393 ^c	3.82		3.59	
3a	S	253	3.78	3.97	3.61	3.77
2a	W	293	3.73		3.54	
2a	S	183 ^b	3.48	3.75	3.41	3.51
5a	W	393 ^c	3.84		3.52	
5a	S	253	3.73	4.07	3.61	3.74

^a Free rotation (W = working); frozen rotation (S = stopped). ^b CD_2Cl_2 . ^c $\text{DMSO}-d_6$. ^d Eight overlapped signals.

2a–5a, in correlation with the ortho, meta (2,6-pyridylene) para substitution of ring **B**, and also for the conformational behavior of monomer **4a**, when compared to dimer **4b**. The ^1H NMR spectra recorded at ambient temperature indicate freezing of the rotation of pyridine ring (**A**) in **4a**, coalescence in **3a** and **5a**, and free rotation of the pyridine ring in **2a**. To observe frozen (stopped rotors) and mobile structures (working rotors), we carried out variable-temperature NMR experiments by both lowering (CDCl_3 or CD_2Cl_2 as solvents) and raising ($\text{DMSO}-d_6$ as solvent) the temperature. During these itineraries, successive coalescences were observed. The barriers [$\Delta G^\ddagger = 11.4 \pm 0.4$ (**2a**); 14.9 ± 0.7 (**3a**); 14.3 ± 0.6 (**5a**); 9.2 ± 0.5 kcal/mol (**4b**); $\Delta G^\ddagger > 20.1$ kcal/mol (**4a**)] of the conformational processes were estimated using the temperatures of coalescence (see Supporting Information) and the chemical shifts measured for the frozen structures. The experimental data show modifications of the rotation barrier similarly with those suggested by the calculated ones. The evolution diagrams obtained by molecular modeling confirm the increasing of the barrier of the rotation of ring **A** in the series of **2a** \ll **5a** $<$ **3a** \ll **4a**. For example, in the spectra of **5a** (Figure 1) recorded in CDCl_3 or $\text{DMSO}-d_6$ at rt, the signals pertaining to the protons of the 1,3-dioxane rings and to the equatorial CH_2 groups at positions 5' and 5'' are in coalescence and are dispersed in the baseline.

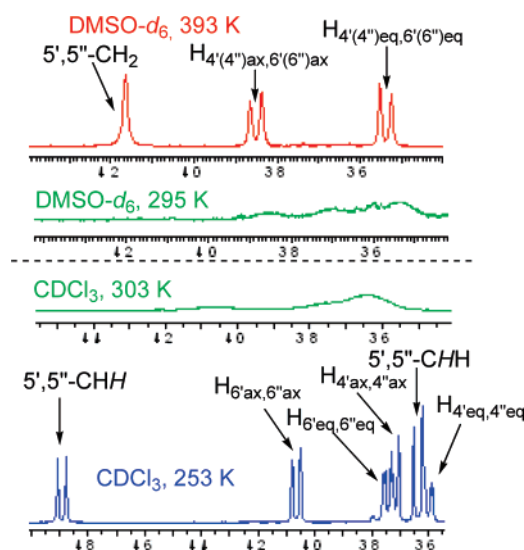


Figure 1. Variable-temperature NMR experiments run with **5a**.

The high-temperature spectrum (393 K; in $\text{DMSO}-d_6$) of **5a**, corresponding to the working *wringer*, shows a single set of signals, comprising one doublet for the equatorial protons ($\delta = 3.52$ ppm) and another doublet for the axial protons ($\delta = 3.84$ ppm) at positions 4'(4'') and 6'(6'') of the 1,3-dioxane rings, and one singlet ($\delta = 4.18$ ppm) for the protons of the equatorial CH_2 groups at positions 5' and 5''. The low-temperature spectrum (253 K; in CDCl_3), corresponding to the stopped half-rotor, is more complicated and exhibits two doublets for the diastereotopic equatorial protons at positions 4'(4'') and 6'(6'') ($\delta_{4'\text{eq},4''\text{eq}} = 3.61$, $\delta_{6'\text{eq},6''\text{eq}} = 3.74$ ppm) and two other doublets for the axial protons at the same positions ($\delta_{4'\text{ax},4''\text{ax}} = 3.73$, $\delta_{6'\text{ax},6''\text{ax}} = 4.07$ ppm). The low-temperature spectrum also shows two doublets with large diastereotopicity for the protons of the CH_2 groups at positions 5' and 5'' ($\delta_{5'\text{a},5''\text{a}} = 3.64$, $\delta_{5'\text{b},5''\text{b}} = 4.89$; $\Delta\delta_{\text{a-b}} = 1.25$ ppm). The NMR spectra of monomer **4a** and of dimer **4b** reveal important differences in their conformational behavior. The NMR spectra of monomer **4a** suggest a frozen structure at rt and do not show modifications in the high-temperature spectra (until 393 K, the limit of the equipment; $\text{DMSO}-d_6$), while the NMR spectra of dimer **4b** reveal the free rotation of the pyridine ring at rt and the frozen structure of the “rotor” at low temperature (180 K). Treatment of cyclophane **5a** with $\text{CF}_3\text{SO}_3\text{Ag}$ generated a tetranuclear coordination complex (as inferred eventually from X-ray data, vide infra) **6a**, which was crystallized from CHCl_3 –pentane. As expected, the ^1H NMR spectrum of **6a** shows major changes relative to the starting ligand **5a**, but a thorough assignment of the signals was not possible so that a structure in solution could not be drawn for the complex.

The solid-state molecular structures of cyclophanes **2a** and **5a**, and of complex **6a** (Figure 2a–d) were obtained by single-crystal X-ray diffractometry. The X-ray analysis of **2a** (Figure 2a) revealed the presence of four slightly different molecular structures in the crystal. Differences could be noted

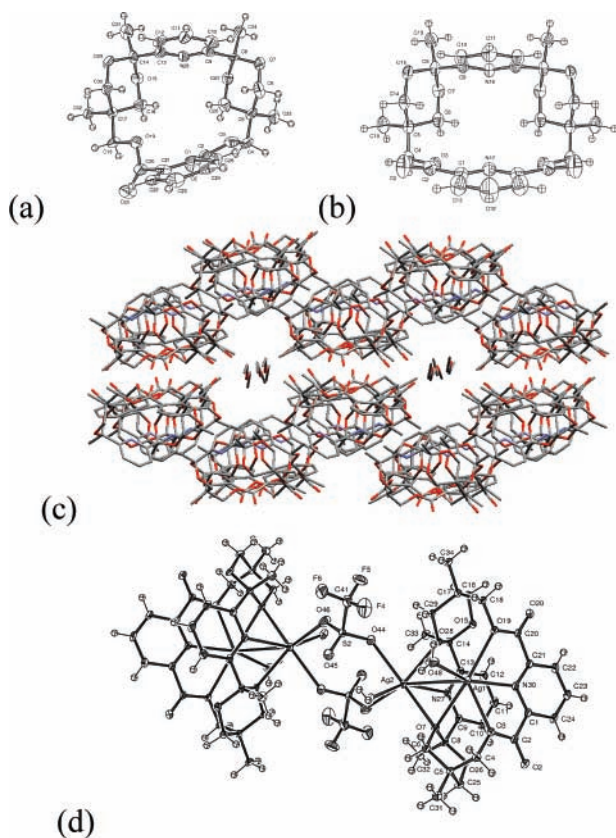


Figure 2. X-ray structures (ORTEP diagrams) of **2a** (a), **5a** (b), **6a** (d), and view of the lattice for **2a** (c).

for the values of the dihedral angles formed by the pyridine ring with the best plane of one of the 1,3-dioxane rings¹¹ (range: 80.39–89.90°) and also for the values of the dihedral angles formed by the two aromatic rings (range: 27.54–32.09°). In addition, the lattice is organized in channels that are filled with diethyl ether molecules (Figure 2c). The molecular structure of **5a** (Figure 2b) shows the axial–orthogonal orientation of the pyridine ring **A** relative to the dioxane rings and its syn orientation with respect to the other pyridine ring (**B**) of the molecule. The X-ray structure of the complex **6a** [(C₂₆H₃₀N₂O₈)₂(OTf)₂(H₂O)₄Ag₄](OTf)₂·2CHCl₃ (Figure 2d) reveals a number of interesting aspects. The complex is formed with the participation of four Ag⁺ cations, two molecules of cyclophane, two triflate anions, and four molecules of water and adopts an unprecedented structure. The silver cations are coordinated differently (giving irregular polyhedrals): two of them are coordinated by the pyridine rings **A** and are denoted as Ag⁺_A, and the other two are coordinated by the pyridine rings **B** and are denoted as Ag⁺_B. The complex is built up around a central eight-membered inorganic ring formed by the Ag⁺_A cations and two bridging triflate anions, and adopting a twisted chair conformation.^{12,13} Each Ag⁺_A cation is heptacoordinated, and

(11) The 1,3-dioxane ring symmetry plane, itself, taken as reference.

besides the two triflate anions, it is also coordinated by a molecule of water and it bridges two oxygen atoms, one from each of the two 1,3-dioxane rings, and the nitrogen atom of the pyridine ring **A** of the same cyclophane molecule, and interacts with Ag⁺_B, too. Each Ag⁺_B cation is hexacoordinated. The two sp³ oxygen atoms of the ester groups, the nitrogen atom of the pyridine ring **B**, one of the oxygen atoms of an 1,3-dioxane ring (all these coordinating atoms belonging to the same cyclophane molecule), and finally, a water molecule completes the coordination sphere of this silver cation.

An interesting feature observed in the crystal structure of **6a** is that the complexation resulted in the inversion of the 1,3-dioxane rings such that in the complex the pyridine ring **A** exhibits equatorial orientations relative to both 1,3-dioxane rings. While in the parent cyclophane the pyridine ring **B** was bridged by equatorial groups, in the complex this pyridine ring is connected to the 1,3-dioxane rings by axial –CH₂OCO– groups. The lattice (see the Supporting Information) also contains two triflate anions for each molecule of complex and shows the formation of channels which are filled with molecules of CHCl₃ (two molecules of solvent for each molecule of complex).

In summary, we report herein the synthesis and structural analysis of new [7.7]cyclophanes and their behavior as molecular *wringers*. The hindrance of the work of these new rotors (2,6-disubstituted pyridine rings) is more severe if the other aromatic ring is bridged through the para positions than if it is connected via the meta (2,6-) or ortho positions. The complexation of cyclophane **5a** with silver cations stopped the rotor and led to an intriguing complex with two silver cations bridged by two triflate anions (forming a eight-membered inorganic cycle), which triggered a dramatic change of conformation of the 1,3-dioxane moieties.

Acknowledgment. AUF (Agence Universitaire de la Francophonie) and “Le Conseil Général de la Région Haute-Normandie” are gratefully acknowledged for the fellowships given to N.B. CNCSIS is acknowledged for the partial financial support of this work (Grant Nos. A1736/2004, T_d 14/2002-2004, and B_d 2003-2005). We thank Dr. Eugen F. Mesaros from Cephalon, Inc., for useful discussions.

Supporting Information Available: Synthesis, procedures, and characterization of the precursors, general experimental data, NMR determination of the barriers of rotation, results of the molecular modeling, copies of the ¹H and ¹³C NMR spectra, CIF file, and a table of the parameters for the crystallographic determinations. This material is available free of charge via the Internet at <http://pubs.acs.org>.

OL0610845

(12) Eliel, E. L.; Wilen, S. H. *Stereochemistry of Organic Compounds*; John Wiley and Sons: Chichester, 1994; p 765.

(13) similar structures are already reported in the literature: (a) Budka, J.; Lhotak, P.; Stibor, I.; Sykora, J.; Cisarova I. *Supramol. Chem.* **2003**, *15*, 353–357 (b) Munakata, M.; Ping Wu L.; Kuroda-Sowa, T.; Maekawa, M.; Suenaga, Y.; Ohta, T.; Konaka, H. *Inorg. Chem.* **2003**, *42*, 2553–2558 (c) Sengupta, P.; Zhang, H.; Son, D. Y. *Inorg. Chem.* **2004**, *43*, 1828–1830.